

IGF-II is regulated by microRNA-125b in skeletal myogenesis

Yejing Ge, Yuting Sun, and Jie Chen

Department of Cell and Developmental Biology, University of Illinois at Urbana-Champaign, Urbana, IL 61801

MicroRNAs (miRNAs) have emerged as key regulators of skeletal myogenesis, but our knowledge of the identity of the myogenic miRNAs and their targets remains limited. In this study, we report the identification and characterization of a novel myogenic miRNA, miR-125b. We find that the levels of miR-125b decline during myogenesis and that miR-125b negatively modulates myoblast differentiation in culture and muscle regeneration in mice. Our results identify IGF-II (insulin-like growth factor 2), a critical regulator of

skeletal myogenesis, as a direct and major target of miR-125b in both myocytes and regenerating muscles, revealing for the first time an miRNA mechanism controlling IGF-II expression. In addition, we provide evidence suggesting that miR-125b biogenesis is negatively controlled by kinase-independent mammalian target of rapamycin (mTOR) signaling both in vitro and in vivo as a part of a dual mechanism by which mTOR regulates the production of IGF-II, a master switch governing the initiation of skeletal myogenesis.

Introduction

During skeletal muscle development, cells from the somites commit to myogenic lineage and progress along the myogenic pathway by proliferation, terminal differentiation, and formation of multinucleated myofibers (Buckingham, 2001). The entire process is guided by various environmental cues and regulated by distinct signaling pathways, resulting in the activation of specific transcription factors and subsequent reprogramming of gene expression (Weintraub, 1993; Lassar and Münsterberg, 1994; Naya and Olson, 1999; Perry and Rudnick, 2000). Skeletal muscle regeneration is one of the adult muscle remodeling processes, which involves satellite cell (or other types of muscle stem cell) activation, proliferation, and differentiation to form new myofibers (Wagers and Conboy, 2005). Muscle regeneration shares a high extent of regulatory mechanisms with embryonic myogenesis (Parker et al., 2003) and serves as an experimental model to study the regulation of skeletal myogenesis in vivo. Myogenesis is also largely recapitulated by in vitro culture of myoblasts, which, in response to serum withdrawal, exit the cell cycle, differentiate, and fuse to form myotubes.

The insulin-like growth factors (IGFs) have long been established to play critical roles in skeletal myogenesis both

during development and in adult muscle remodeling (Florini et al., 1991a, 1996). IGF-II, an embryonic regulator of myogenesis and an autocrine factor that initiates myoblast differentiation in vitro (Florini et al., 1991b), is regulated at the transcriptional level through a muscle-specific enhancer by mammalian target of rapamycin (mTOR) signaling (Erbay et al., 2003). IGF-II translation has also been shown to be regulated by an RNA-binding protein, LIN-28, during skeletal myogenesis (Polesskaya et al., 2007). Given its critical role in the initiation of myogenesis, it would not be surprising if the production of IGF-II during myogenesis were under additional modes of regulation yet to be discovered.

MicroRNAs (miRNAs), ~22-nt noncoding RNAs regulating gene expression at posttranscriptional levels, have emerged as key regulators for many developmental processes (Bushati and Cohen, 2007; Bartel, 2009), including skeletal myogenesis. The central role of miRNAs in skeletal muscle development has been demonstrated by the detrimental consequence of *Dicer* deletion in embryonic skeletal muscle (O'Rourke et al., 2007). Several muscle-specific miRNAs that control various aspects of myogenesis have been identified and characterized (Callis et al., 2008; Williams et al., 2009). The best studied are the miR-1/206

Correspondence to Jie Chen: jiechen@illinois.edu

Abbreviations used in this paper: AI, after injury; LNA, locked nucleic acid; MHC, myosin heavy chain; miRNA, microRNA; mTOR, mammalian target of rapamycin; shRNA, short hairpin RNA; TA, tibialis anterior; UTR, untranslated region.

© 2011 Ge et al. This article is distributed under the terms of an Attribution–Noncommercial–Share Alike–No Mirror Sites license for the first six months after the publication date (see <http://www.rupress.org/terms>). After six months it is available under a Creative Commons license [Attribution–Noncommercial–Share Alike 3.0 Unported license, as described at <http://creativecommons.org/licenses/by-nc-sa/3.0/>].

Supplemental material can be found at:
<http://doi.org/10.1083/jcb.201007165>

and miR-133 families, which regulate fundamental processes of myogenesis including myoblast/satellite cell proliferation and differentiation under the control of myogenic transcription factors (Williams et al., 2009 and references therein). Additional miRNAs reported to function in skeletal myogenesis include miR-24 (Sun et al., 2008), miR-26a (Wong and Tellam, 2008), miR-27b (Crist et al., 2009), miR-29 (Wang et al., 2008), miR-181 (Naguibneva et al., 2006b), miR-214 (Juan et al., 2009), miR-221/222 (Cardinali et al., 2009), miR-486 (Small et al., 2010), and miR-208b/miR-499 (van Rooij et al., 2009). Direct targets in muscles have been identified for some of these miRNAs but not others. It would be reasonable to speculate that more myogenic miRNAs are yet to be discovered.

miR-125b, as well as its paralogue miR-125a, is the homologue of *Caenorhabditis elegans* lin-4, the first miRNA reported (Lee et al., 1993). Both miR-125a and miR-125b are highly expressed in mouse brains, but only miR-125b is easily detectable in several other tissues, including heart, lung, spleen, and skeletal muscle (Lagos-Quintana et al., 2002). miR-125 has been implicated in neuronal differentiation of mouse P19 cells by targeting the RNA-binding protein LIN-28 (Wu and Belasco, 2005), and it also promotes neuronal differentiation in human cells by suppressing multiple targets (Le et al., 2009b). Moreover, it has been demonstrated that miR-125b targets p53 in stress-induced apoptosis (Le et al., 2009a). However, a function for miR-125b in skeletal muscle has never been reported despite its notable expression in the muscle. In this study, we report that miR-125b negatively modulates myoblast differentiation in vitro and muscle regeneration in vivo. We identify IGF-II as the molecular target of miR-125b in skeletal myogenesis. Furthermore, our results suggest that mTOR signaling controls the levels of miR-125b during myogenesis both in vitro and in vivo.

Results

miR-125b is down-regulated during myoblast differentiation in vitro and muscle regeneration in vivo

In an miRNA profiling that we had previously performed (Sun et al., 2010), miR-125b was found to be down-regulated during C2C12 myoblast differentiation. The closely related miR-125a was detected at a much lower level, which is consistent with the findings from other studies (Chen et al., 2006; Inose et al., 2009), and unchanged upon differentiation (Sun et al., 2010). To confirm the down-regulation of miR-125b observed in our microarray experiments, we examined miR-125b levels by quantitative RT-PCR (qRT-PCR) in C2C12 cells induced to differentiate by serum withdrawal, which formed mature myotubes by day 3 as we had previously reported (Erbay et al., 2003). Indeed, miR-125b levels decreased by ~30% and 50% by days 2 and 3 of differentiation, respectively (Fig. 1 A). A similar decrease of miR-125b levels was observed during differentiation of mouse primary myoblasts (Fig. 1 B). This decrease of miR-125b during myoblast differentiation was observed by others as well (Polesskaya et al., 2007), although its functional significance remained unknown. A recent study suggested that cell-cell contact could activate miRNA biogenesis globally

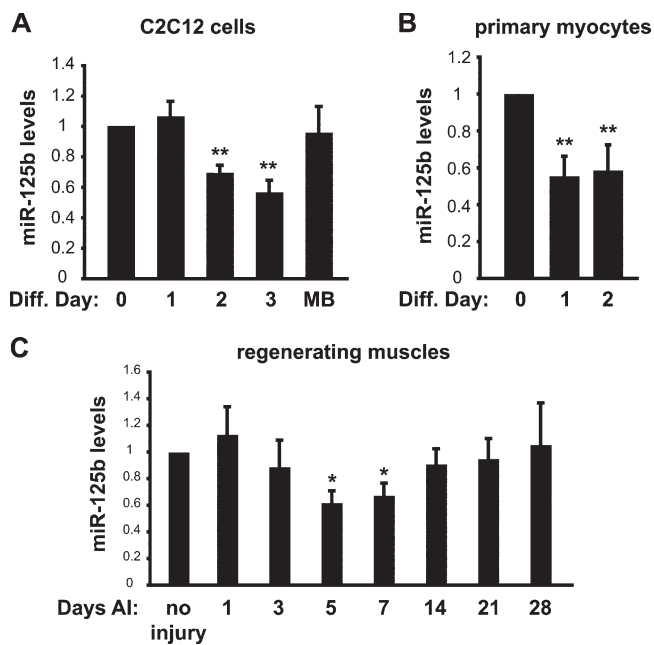


Figure 1. miR-125b is down-regulated during myoblast differentiation and muscle regeneration. (A and B) C2C12 cells (A) and mouse primary myoblasts (B) were induced to differentiate at 100% and 60–70% confluence, respectively. Total RNA was isolated from the differentiating cells on various days as indicated (diff. day) and subjected to analysis by qRT-PCR to determine the relative levels of mature miR-125b. Proliferating C2C12 myoblasts (MB) at 60% confluence were also examined in A. (C) Regeneration of TA muscles in mouse was induced by BaCl₂ injury. On various days AI, total RNA was isolated from the TA muscles and subjected to analysis by qRT-PCR to determine the relative levels of mature miR-125b. Saline injection into contralateral TA muscles served as “no injury” control. The data in A and B are mean ± SD from three to four independent experiments. The data in C are mean ± SD with four mice per time point. One-sample *t* test was performed to compare each data point with the control (0 h or no injury). *, *P* < 0.05; **, *P* < 0.01.

(Hwang et al., 2009). Unlike primary myoblasts, which were differentiated at subconfluence, C2C12 cell differentiation was typically initiated at 100% confluence in our experiments. To assess any potential change in miR-125b levels caused by cell-cell contact, we compared confluent culture (differentiation day 0) and proliferating myoblasts at ~60% confluence and found no difference in miR-125b levels (Fig. 1 A). Thus, miR-125b biogenesis did not seem to be influenced by cell density under our experimental conditions.

Next, we assessed miR-125b expression during skeletal muscle regeneration in vivo in a mouse muscle injury model. We have recently shown that barium chloride (BaCl₂) injection into the tibialis anterior (TA) muscle induces acute and severe myofiber degeneration on day 1 after injury (AI), followed by myofiber regeneration that reaches completion by days 21–28 AI (Ge et al., 2009), which is consistent with previous studies by others (Caldwell et al., 1990; McArdle et al., 1994). The levels of miR-1 and miR-206, two of the best-studied myogenic miRNAs, decreased on day 3 AI and then increased during the regeneration time course (Fig. S1), in full agreement with reported observations (Greco et al., 2009; Chen et al., 2010). As shown in Fig. 1 C, miR-125b levels declined on days 5–7 AI, which is a period of active new myofiber formation (Ge et al., 2009), and returned to the basal level after that. This temporary

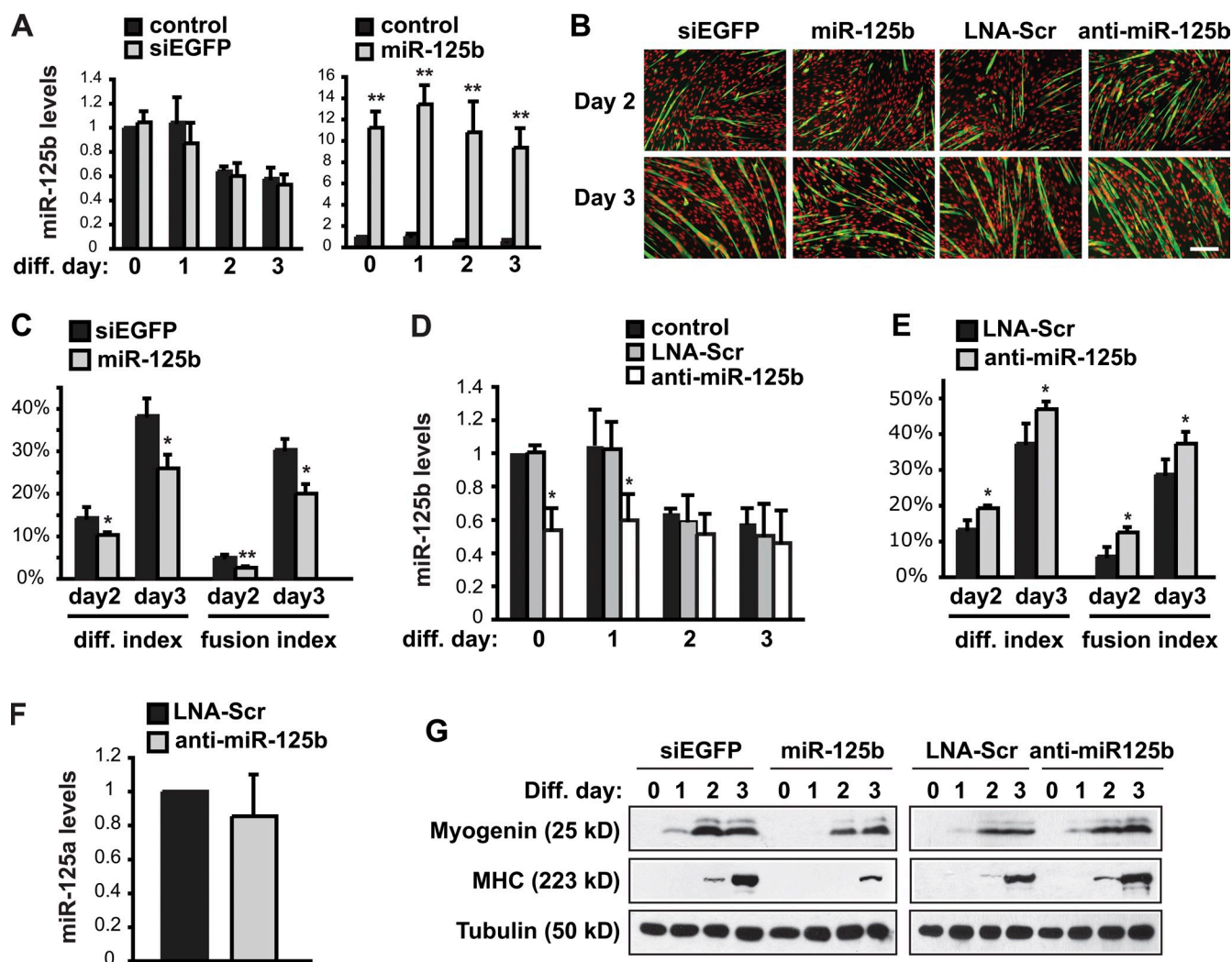


Figure 2. miR-125b negatively regulates myoblast differentiation. C2C12 myoblasts were transfected with 50 nM RNA duplexes or LNA-containing oligonucleotides and then were induced to differentiate 1 d later for 3 d. An siRNA against EGFP (siEGFP) and an LNA oligonucleotide with scrambled sequence (LNA-Scr) served as negative controls for miR-125b duplex and anti-miR-125b, respectively. (A and D) Relative miR-125b levels were measured by qPCR in nontransfected cells (control) and cells transfected with various oligonucleotides, as indicated, during the course of differentiation (diff.). (B) The differentiated cells were fixed, and immunostained for MHC (green) and DAPI (red). Bar, 100 μ m. (C and E) Differentiation and fusion indexes were quantified. (F) Relative miR-125a levels were measured by qPCR 1 d after transfection of LNA oligonucleotides (same as diff. day 0). (G) Western blot analysis of cells treated as described in A. In B and G, representative results of at least three independent experiments are shown. All quantitative data are shown as mean \pm SD from three to four independent experiments. For the qPCR data (A, D, and F), one-sample *t* tests were performed to compare each data point against control on day 0 (A and D) or between LNA-Scr and anti-miR-125b (F). For the differentiation and fusion index data (C and E), paired *t* tests were performed to compare data within each time point. *, *P* < 0.05; **, *P* < 0.01.

decrease of miR-125b expression during regeneration *in vivo* is in line with the pattern of miR-125b expression during myoblast differentiation, which suggests a potentially negative role of miR-125b in myogenesis.

miR-125b negatively regulates myoblast differentiation and muscle regeneration

To investigate a potential role of miR-125b in myoblast differentiation, we introduced a synthetic RNA duplex of miR-125b into C2C12 myoblasts, which were then induced to differentiate. As shown in Fig. 2 A, delivery of this duplex was highly effective, increasing cellular miR-125b levels by >10-fold. This exogenous miR-125b dampened C2C12 differentiation, as indicated by decreased myotube formation (Fig. 2 B). Quantification of the myotubes revealed significant decreases in both

differentiation index (percentage of nuclei in myosin heavy chain [MHC]-positive cells) and fusion index (percentage of nuclei in myocytes with at least two nuclei) as shown in Fig. 2 C. We also introduced a locked nucleic acid (LNA)-containing antisense miR-125b oligonucleotide, anti-miR-125b (Naguibneva et al., 2006a), into C2C12 cells to antagonize endogenous miR-125b. An LNA-containing oligonucleotide of a scrambled sequence with no complementarity to any known miRNAs served as a negative control. Anti-miR-125b reduced the cellular level of miR-125b by \sim 50% before the natural decline of miR-125b to a similar extent (Fig. 2 D), and this was accompanied by enhanced myotube formation (Fig. 2 B), as confirmed by increased differentiation and fusion indexes (Fig. 2 E). Anti-miR-125b did not change the cellular level of miR-125a (Fig. 2 F), validating the specificity of the antisense oligonucleotide. Two myogenic

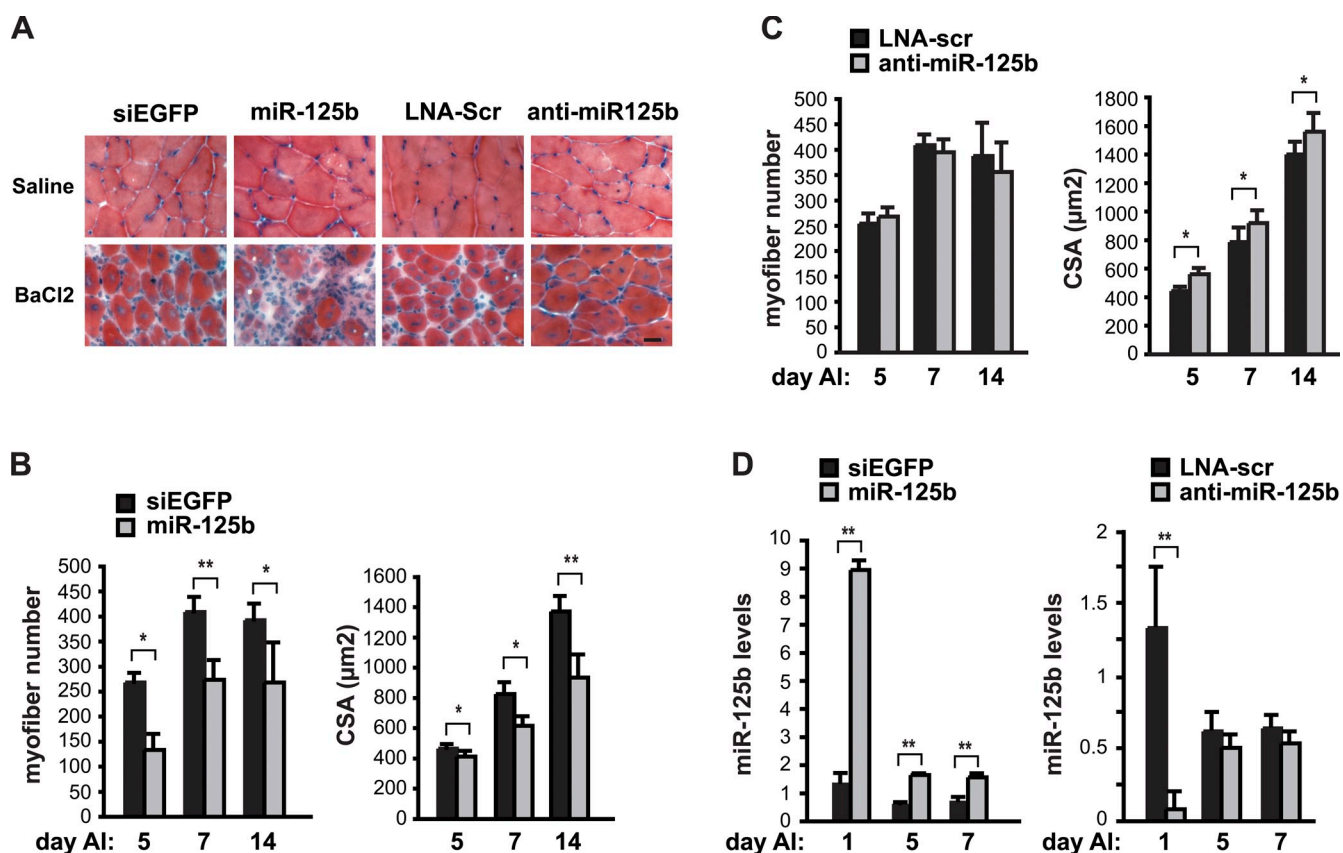


Figure 3. miR-125b negatively regulates skeletal muscle regeneration. Mouse TA muscles were injured with BaCl₂ injection, and oligonucleotides (same RNA duplexes and LNA-modified oligonucleotides as in Fig. 2) were coinjected at 0.2 μg/μl as indicated. On various days AI, the TA muscles were isolated and either cryosectioned or extracted for RNA. As controls, saline was injected instead of BaCl₂, together with the oligonucleotides, into the contralateral limb TA muscles. (A) Cross sections of TA muscle on day 7 AI were stained with H&E. A portion of the regenerating area is shown to provide a representative view. Bar, 50 μm. (B and C) On various days AI, regenerating myofibers (identified by their central nuclei on H&E-stained sections) were counted within a 614,400-μm² view for each sample. Cross section areas (CSA) of regenerating myofibers were quantified. At least 100 regeneration myofibers were measured on each muscle section. Note that the regenerating muscle area included for quantitative analysis in B and C was ~10 times larger than that shown in A. (D) miR-125b in oligonucleotide-injected and injured muscles on various days AI was measured by qPCR. Relative miR-125b levels are shown with “no injury” sample set at 1 (see Fig. 1C). All results shown are mean ± SD (*n* = 5 mice for each data point in B and C; *n* = 3 mice for each data point in D). Paired *t* test was performed to compare each pair of data as indicated. *, *P* < 0.05; **, *P* < 0.01.

differentiation markers, myogenin (early) and MHC (late), were both expressed at levels that correlated well with morphological differentiation upon miR-125b or anti-miR-125b expression (Fig. 2 G). The milder effect of anti-miR-125b on differentiation compared with miR-125b is consistent with its moderate impact on cellular miR-125b levels. Delivery of these oligonucleotides into C2C12 cells by transfection was assessed using the fluorescently labeled Dy547-cel-miR-67 (RNA duplex) and FAM-anti-miR (single-stranded RNA), and the efficiency was ~90% and ~75%, respectively (Fig. S2 A). The degree of oligonucleotide up-take varied among the transfected cells for both types of probes (Fig. S2 A), and it is possible that maximal manipulation of miR-125b did not occur in all transfected cells. Nevertheless, the inverse relationship between miR-125b levels and degrees of myoblast differentiation clearly evident from our data suggests that miR-125b negatively regulates myogenic differentiation.

To probe a possible role of miR-125b in myoblast proliferation, we examined BrdU incorporation in C2C12 cells transfected with synthetic miR-125b or anti-miR-125b. As shown in Fig. S2 B, manipulation of miR-125b levels had no effect on the proliferation of myoblasts. Furthermore, introduction of

miR-125b or anti-miR-125b did not change the cell number by the end of differentiation (Fig. S2 C). Thus, miR-125b does not appear to regulate myoblast proliferation or survival but rather has a specific role in myoblast differentiation.

To probe the function of miR-125b in muscle regeneration in vivo, we introduced miR-125b duplex and, separately, LNA-containing anti-miR-125b into the muscle injury site by coinjecting the oligonucleotides with BaCl₂. Muscle regeneration was then examined on days 5, 7, and 14 AI. Representative cross sections of regenerating muscle on day 7 AI are shown in Fig. 3 A; exogenous miR-125b impaired regeneration, as indicated by the incomplete restoration of muscular structure at the injury site. Injection of any of the oligonucleotides in the absence of BaCl₂ had no detectable effect on the muscles (Fig. 3 A, saline panels). Regenerating myofibers, characterized by their centrally localized nuclei, were quantified, and the results revealed a reduction in the number of regenerating myofibers as well as a smaller mean myofiber size upon injection of miR-125b duplex on days 5, 7, and 14 AI (Fig. 3 B). In contrast, anti-miR-125b injection enhanced muscle regeneration as indicated by the modest, nonetheless statistically significant, increase in regenerating myofiber

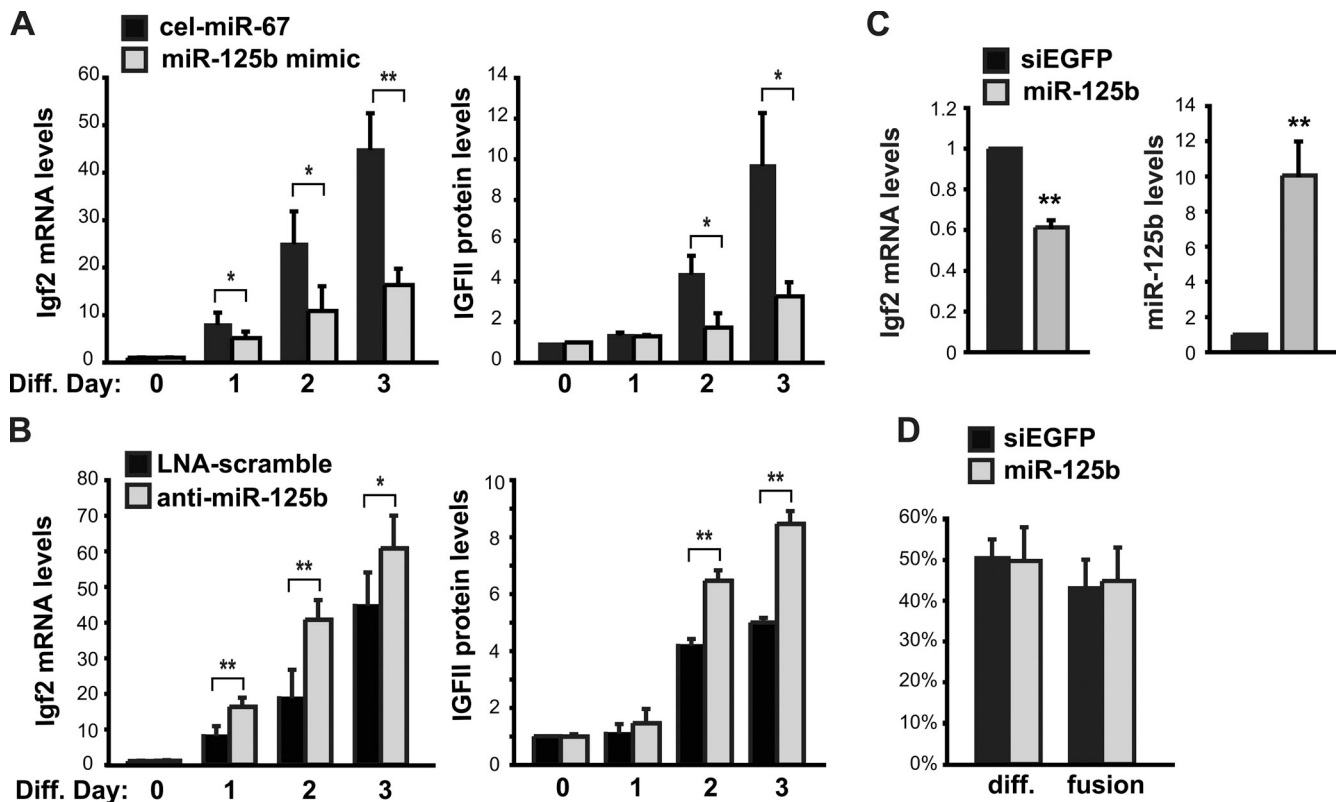


Figure 4. IGF-II levels are regulated by miR-125b during myoblast differentiation. (A and B) C2C12 myoblasts were transfected with 50 nM miRIDIAN miR-125b mimic (A) or LNA-containing anti-miR-125b (B) and, after 1 d, induced to differentiate for up to 3 d. As negative controls, miRIDIAN cel-miR-67 and LNA-scramble were transfected side by side with miR-125b mimic and anti-miR-125b, respectively. Cells were lysed at various time points for RNA isolation, followed by qRT-PCR to measure IGF-II mRNA levels (left). At the same time, cell media were collected, and IGF-II protein levels were measured by ELISA (right). (C) On day 2 of differentiation, C2C12 myocytes were transfected with 50 nM miR-125b duplex or siEGFP (control). Total RNA was extracted 12 h later and subjected to qPCR analysis for Igf2 mRNA (left) and miR-125b (right). (D) C2C12 myoblasts were transfected with 50 nM miR-125b duplex or siEGFP (control) as indicated and induced to differentiate for 3 d in the presence of 300 ng/ml recombinant IGF-II. The differentiation (diff.) and fusion indexes were measured. All data shown are mean \pm SD from three independent experiments. Paired *t* test was performed to compare each pair of data in A, B, and D. One-sample *t* test was performed for data in C. *, *P* < 0.05; **, *P* < 0.01.

size on days 5, 7, and 14 AI (Fig. 3 C). The regenerating myofiber number was not further increased by anti-miR-125b at any time during regeneration (Fig. 3 C), likely because the natural decline of miR-125b (Fig. 1 C) was sufficient to allow new myofiber formation to reach saturation at this time point (Ge et al., 2009). Injection of the two negative control oligonucleotides (siEGFP and LNA-scramble) did not have any effect on the normal regenerating myofiber number and size (unpublished data). The more modest effects of anti-miR-125b compared with duplex miR-125b could also be attributed to the difference in delivery efficiency and/or stability of the two types of oligonucleotides in muscles. Indeed, after a dramatic change of miR-125b levels in both miR-125b- and anti-miR-125b-injected muscles on day 1 AI, miR-125b remained elevated to a similar level as in noninjured muscles even on day 7 AI, whereas anti-miR-125b injection no longer had an effect on miR-125b levels by day 5 AI (Fig. 3 D). We did not measure miR-125b levels beyond day 7 AI because it was unlikely that the injected oligonucleotides would remain stable in vivo for an extended time. Nevertheless, it is conceivable that a difference in myofiber formation could be observed at later time points even when the miR-125b level was no longer detectably changed, as an impact on the early stage of regeneration could change the entire time course of regeneration.

In conclusion, consistent with its role in myoblast differentiation, miR-125b negatively impacts skeletal muscle regeneration in vivo. This is the first time that miR-125b is assigned a function in skeletal myogenesis.

miR-125b regulates IGF-II expression during myogenesis

We next asked what the molecular target or targets of miR-125b in myogenesis might be. miRNAs are believed to exert their function mostly by imperfect pairing with the 3' untranslated region (UTR) of target mRNAs. A seed region at the 5' end of the mature miRNA (starting at nt 2, up to nt 9) in the miRNA-mRNA duplex has been found to be largely responsible for effective miRNA targeting (Stark et al., 2003; Krek et al., 2005; Lewis et al., 2005), although seedless targeting has also been reported (Juan et al., 2009; Lal et al., 2009; Shin et al., 2010). Computational target prediction using miRanda, TargetScan, and PicTar yielded >1,000 potential gene targets for miR-125b. Because miRNAs are known to induce target mRNA degradation (Baek et al., 2008; Guo et al., 2010), we looked for predicted miR-125b targets that were up-regulated at the mRNA level during myoblast differentiation, taking advantage of gene expression profiles in differentiating C2C12 cells that we had

previously generated (Park and Chen, 2005). This yielded a list of 11 predicted genes (Table S1). Among them, *Igf2* emerged as the most attractive candidate, as it has well-established roles in skeletal myogenesis (Florini et al., 1991a, 1996). It is noted that although the predicted miR-125b targeting sequence is identical in rat and mouse *Igf2* genes, the human gene is different by 2 nt in the seed region (Fig. S3). However, the overall sequence conservation in the miR-125b target region between rodent and human *Igf2* is high, and the human gene has potentially two more base pairings with miR-125b outside of the 6-mer seed region (Fig. S3). Seedless targeting of human *Igf2* by miR-125b is possible, although it cannot be reliably predicted. We decided to focus on the mouse gene in this study as the relevant experimental systems, both in vitro and in vivo, were readily available.

To examine the possibility of miR-125b targeting IGF-II, we asked whether miR-125b regulated IGF-II expression. Both mRNA and protein levels of IGF-II increased during C2C12 differentiation (Fig. 4 A, black bars) as previously reported (Florini et al., 1991b; Erbay et al., 2003), which correlated well with the drop of miR-125b levels at the same time (compare Fig. 4 A with Fig. 1 A). More importantly, both mRNA and protein levels of IGF-II were reduced by 60–70% on days 2 and 3 of differentiation when a chemically modified miR-125b mimic (miRIDIAN) was transfected into the cells (Fig. 4 A). Native miR-125b duplex exerted a similar but less pronounced effect on IGF-II levels (unpublished data). Conversely, anti-miR-125b enhanced IGF-II expression at both mRNA and protein levels (Fig. 4 B). The degree of enhancement (1.3–2-fold) was quite remarkable considering that IGF-II was already up-regulated drastically during normal differentiation. The inhibition of IGF-II by miR-125b is unlikely caused by a secondary effect of miR-125b suppression of differentiation, as miR-125b duplex transfected into day 2 differentiated C2C12 myotubes potently inhibited IGF-II levels only after 12 h (Fig. 4 C).

If IGF-II were a major functional target of miR-125b, exogenous IGF-II would be expected to override the negative effect of miR-125b on differentiation. Indeed, differentiation of C2C12 cells, as measured by differentiation and fusion indexes, was no longer sensitive to miR-125b duplex when the cell medium was supplemented with recombinant IGF-II (Fig. 4 D). This suggests that IGF-II may mediate a significant portion of miR-125b's negative function in myogenesis, even if *Igf2* is not the sole target of miR-125b.

IGF-II expression increases acutely during injury-induced muscle regeneration, and it peaks around 5–7 d AI before declining (Paoni et al., 2002; Ge et al., 2009), which inversely correlates with the expression pattern of miR-125b in regenerating muscles (Fig. 1 C). Coinjection of miR-125b duplex with the injury-inducing BaCl₂ lowered *Igf2* mRNA levels by ~45% on day 7 AI, and, conversely, coinjection of anti-miR-125b increased *Igf2* mRNA by ~35% (Fig. 5). Injection of those oligonucleotides in the absence of BaCl₂ did not affect *Igf2* levels (Fig. 5, noninjured). The efficacy of delivering oligonucleotides into muscles might not be optimal (Fig. 3 D), but the observed effects are significant and fully consistent with miR-125b targeting IGF-II during muscle regeneration in vivo.

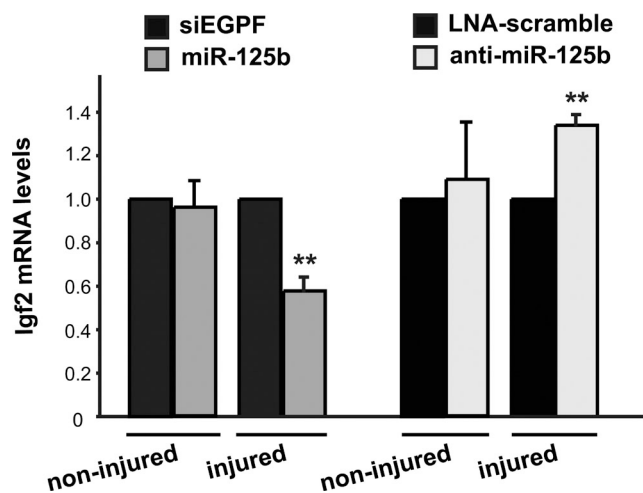


Figure 5. **IGF-II levels are regulated by miR-125b during muscle regeneration.** Mouse TA muscles were injected with oligonucleotides alone (non-injured) or together with BaCl₂ (injured) as described in the legend for Fig. 3. On day 7 AI, the TA muscles were isolated for RNA extraction, followed by qRT-PCR assays to measure *Igf2* mRNA levels. Data shown are mean \pm SD with three mice per data point. One-sample *t* test was performed to compare each pair of data. **, *P* < 0.01.

The 3' UTR of *Igf2* is targeted by miR-125b

The 3' UTR of *Igf2* was predicted to contain a single miR-125b target site with complete complementarity in the seed region (Fig. 6 A), starting at nt 2670 of the 3048-bp 3' UTR. It is important to note that the major isoforms of *Igf2* mRNA in C2C12 cells, as well as in embryonic skeletal muscles, all have 3' UTR containing this putative miR-125b target site (Rosen et al., 1993). To directly examine the possibility of miR-125b targeting *Igf2* 3' UTR, we constructed a reporter with the entire *Igf2* 3' UTR inserted at the 3' end of the luciferase gene. We first tested the effect of miR-125b on this reporter in HEK293 cells, a non-myogenic cell line which has undetectable levels of miR-125b (Wu et al., 2006; unpublished data). As shown in Fig. 6 B, transfected miR-125b duplex drastically inhibited the reporter activity, whereas it had no effect on the control reporter without the 3' UTR (vector). Most importantly, when the predicted miR-125b seed region in the 3' UTR was mutated, the mutant reporter no longer responded to miR-125b (Fig. 6 B), strongly suggesting that the predicted site is a bona fide target of miR-125b and it is solely responsible for miR-125b targeting of the *Igf2* 3' UTR.

We also examined the reporters in C2C12 cells and found that activity of the wild-type reporter increased steadily during differentiation (Fig. 6 C, black bars), which is consistent with activation of IGF-II expression through desuppression of its 3' UTR. The miR-125b site mutant reporter displayed a constant activity unchanged by the differentiation status of the cells (Fig. 6 C, gray bars), suggesting that miR-125b is most likely a major, if not the only, suppressor of the *Igf2* 3' UTR. Interestingly, the mutant reporter activity was at the same level as the wild-type reporter on day 3 of differentiation, even though ~50% miR-125b remained in the cell (Fig. 1 A). This might suggest that the decreased miR-125b level had reached below the threshold for reporter inhibition. However, comparison of

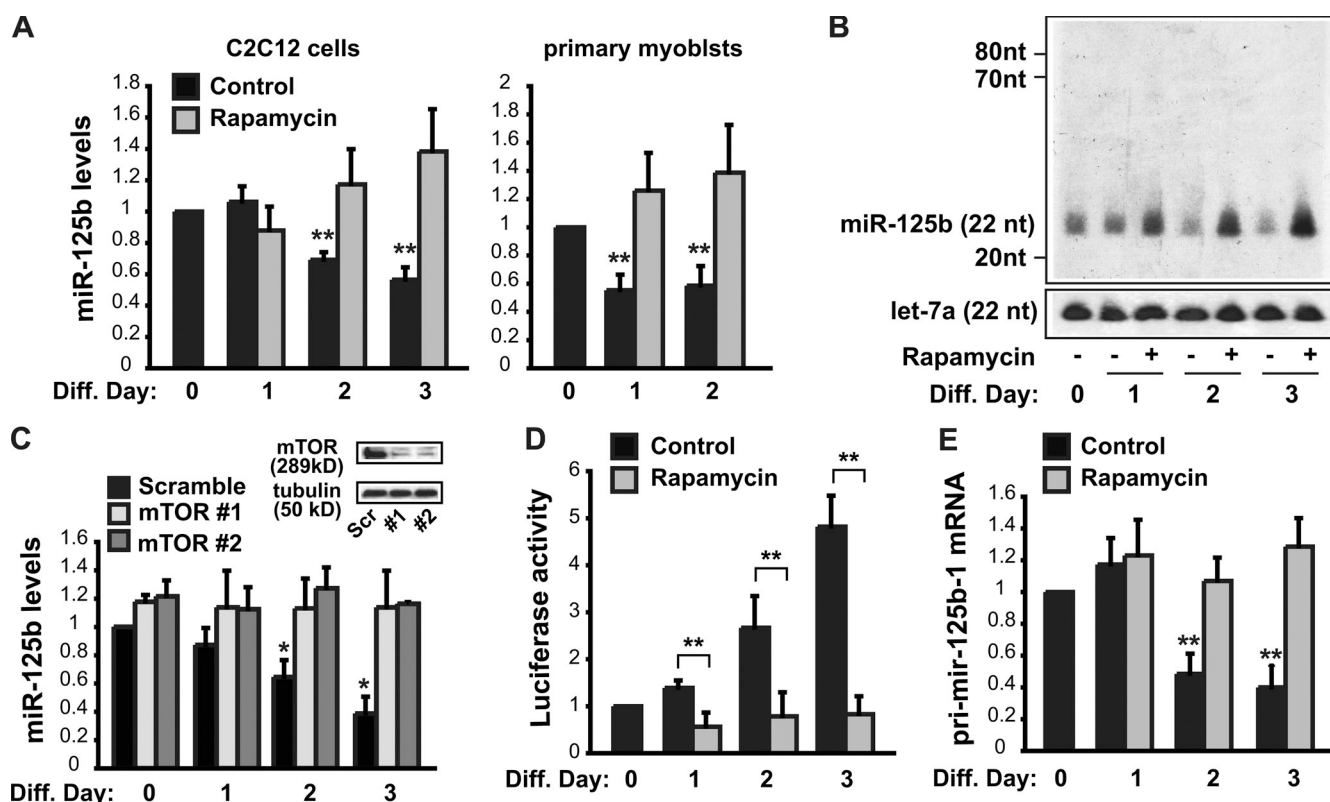


Figure 7. mTOR controls miR-125b levels during myoblast differentiation. (A) C2C12 cells and mouse primary myoblasts were induced to differentiate in the absence or presence of 50 nM rapamycin. Total RNA was isolated from the differentiating cells on various days as indicated (diff. day) and subjected to analysis by qRT-PCR to determine the relative levels of mature miR-125b. (B) RNA samples prepared from C2C12 cells as in A were subjected to Northern blot analysis for miR-125b and let-7a as a control. Pre-miR-125b species (71 and 77 nt) were not detected on the blot. (C) C2C12 cells were transfected with lentiviruses expressing two independent mTOR shRNAs and a scrambled (Scr) hairpin sequence as negative control. After puromycin selection, the cells were treated as in A. The inset shows Western blot results confirming mTOR knockdown. (D) C2C12 cells were transfected with the IGF2 3' UTR reporter and then induced to differentiate in the absence or presence of 50 nM rapamycin. The cells were lysed at the indicated times, and luciferase assays were performed. (E) C2C12 cells were treated as in A, and total RNA was subjected to qRT-PCR analysis for pri-miR-125b-1. All data are mean \pm SD of three independent experiments. Paired *t* test was performed to compare control and rapamycin-treated samples at each time point in D. For the rest of the data, one-sample *t* test was performed to compare each data point with the control (0 h). *, *P* < 0.05; **, *P* < 0.01.

levels of miR-125b primary transcripts (pri-miR-125b). Two genes encode miR-125b at distinct chromosomal loci: *mir-125b-1* and *mir-125b-2*. Although we were unable to detect pri-miR-125b-2 by qRT-PCR, we observed a decrease of pri-miR-125b-1 during differentiation that mirrored the decline of mature miR-125b and was prevented by rapamycin treatment (Fig. 7 E). These data, together with the fact that precursor miR-125b (pre-miR-125b) was not detectable by Northern blot analysis at any point of the differentiation (Fig. 7 B), imply that miR-125b biogenesis during myogenic differentiation is unlikely to be regulated at pri-miR-125b or pre-miR-125b processing. Instead, our observations suggest that miR-125b is regulated at the transcriptional level under the control of mTOR signaling.

Because mTOR signaling regulates IGF-II transcription in a noncanonical manner that is independent of mTOR kinase activity (Erbay et al., 2003), we decided to probe the kinase dependence of mTOR regulation of miR-125b in myoblast differentiation, taking advantage of C2C12 cell lines stably expressing rapamycin-resistant (RR) and rapamycin-resistant/kinase-inactive (RR/KI) mTOR (Erbay et al., 2003). In contrast to parental C2C12 cells, in which rapamycin treatment prevented miR-125b down-regulation during differentiation (Fig. 7 A),

RR-mTOR cells displayed miR-125b down-regulation resistant to rapamycin (Fig. 8 A), confirming that the effect of rapamycin was mediated by mTOR. Remarkably, the RR/KI-mTOR cells behaved identically to the RR-mTOR cells in preserving miR-125b regulation in the presence of rapamycin (Fig. 8 B), indicating that the kinase activity of mTOR is not required. S6K1 is a major target of mTOR kinase in the regulation of cell growth (Fingar et al., 2002) but has been shown to be dispensable for mTOR regulation of IGF-II expression during myogenesis (Erbay et al., 2003). We found that knockdown of S6K1 had no effect on the regulation of miR-125b during differentiation (Fig. 8 C), which is consistent with kinase-independent mTOR regulation of miR-125b and IGF-II.

To seek in vivo validation of the aforementioned observations, we examined the effect of rapamycin on miR-125b levels in regenerating muscles. We found that the transient decrease of miR-125b during muscle regeneration in wild-type mice (days 5 and 7 AI) was prevented by rapamycin administration (Fig. 9 A). This rapamycin sensitivity was absent in transgenic mice expressing muscle-specific RR-mTOR (Fig. 9 B), which displayed rapamycin-resistant muscle regeneration (Ge et al., 2009), validating the notion that rapamycin specifically targets

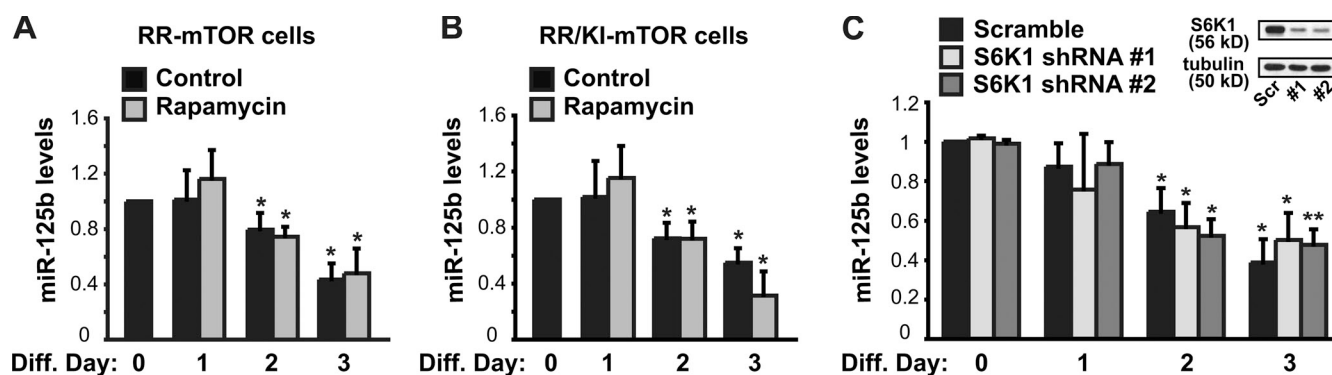


Figure 8. **mTOR regulates miR-125b levels in myoblasts in a kinase- and S6K1-independent manner.** (A and B) C2C12 cells stably expressing RR-mTOR (A) or RR/KI-mTOR (B) were induced to differentiate in the absence or presence of 50 nM rapamycin. Total RNA was isolated from the differentiating cells on various days as indicated (diff. day) and subjected to analysis by qRT-PCR to determine the relative levels of mature miR-125b. (C) C2C12 cells were transduced with lentiviruses expressing two independent S6K1 shRNAs and a scrambled (Scr) hairpin sequence as negative control. After puromycin selection, the cells were treated as in A and B. The inset shows Western blot results confirming S6K1 knockdown. One-sample *t* test was performed to compare each data point with the control (0 h). *, $P < 0.05$; **, $P < 0.01$. Paired *t* tests were also performed to compare samples within each time point, i.e., control with rapamycin on each day in A and B and S6K1 shRNA with scramble in C. No significant difference was found.

mTOR in the regenerating muscle. Strikingly, RR/KI-mTOR transgenic muscles, which we had previously shown to have normal myofiber formation but impaired fiber growth during regeneration in the presence of rapamycin (Ge et al., 2009), also displayed rapamycin-resistant miR-125b down-regulation during regeneration (Fig. 9 C), indistinguishable from RR-mTOR muscles. Therefore, we conclude that kinase-independent mTOR signaling is upstream of miR-125b biogenesis during skeletal myogenesis both in vitro and in vivo.

Discussion

Our study has identified the first miRNA regulator of IGF-II in skeletal myogenesis and revealed a novel function of miR-125b in the negative control of myoblast differentiation in vitro and muscle regeneration in vivo. Although it is possible that other miRNAs are yet to be identified to target IGF-II in myogenesis, our observation that mutation of the seed region of the single predicted miR-125b target site abolished the regulation of the

full-length Igf2 3' UTR reporter during myoblast differentiation (Fig. 6 C) strongly suggests that miR-125b is a major, if not the only, miRNA regulator of IGF-II through its 3' UTR. Furthermore, we show that the levels of miR-125b are controlled by mTOR signaling, shedding light on the myogenic regulation of miR-125b biogenesis and uncovering an additional mechanism by which IGF-II production is regulated by mTOR during myogenesis (Fig. 10).

The functions of mammalian miR-125b and its targets have been reported in several cellular contexts (Wu and Belasco, 2005; Le et al., 2009a,b), but our findings unravel for the first time a myogenic role for miR-125b and a new target, IGF-II. LIN-28, an RNA-binding protein, has been shown to regulate IGF-II translation during myogenesis through the recruitment of IGF-II mRNA to polysomes (Polesskaya et al., 2007). Interestingly, Lin-28 is targeted by lin-4 (miR-125b homologue) in *C. elegans* (Moss et al., 1997) and by miR-125 in mouse neuronal cells (Wu and Belasco, 2005). Thus, it is formally possible that miR-125b regulation of IGF-II during myogenesis may be through targeting

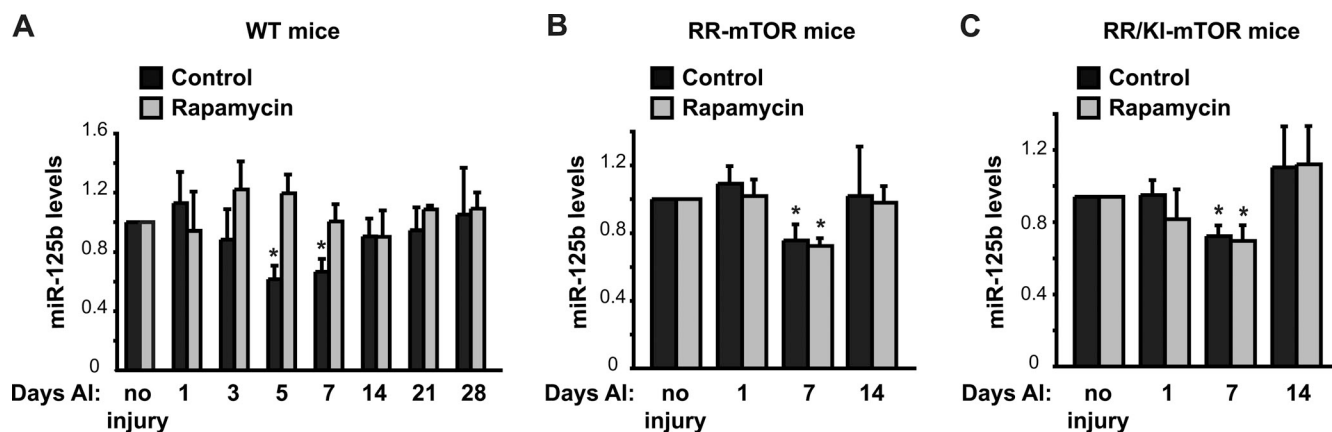


Figure 9. **mTOR regulates miR-125b levels in regenerating muscles in a kinase-independent manner.** (A) TA muscles of wild-type (WT) mice were injected with BaCl₂, and the contralateral muscles were injected with saline as controls (no injury), followed by systemic administration of rapamycin daily from day 1 AI. On various days AI, total RNA was isolated from the TA muscles and subjected to analysis by qRT-PCR to determine the relative levels of mature miR-125b. (B and C) Transgenic mice expressing RR-mTOR (B) or RR/KI-mTOR (C) in skeletal muscle were treated as described in A. All data shown are mean \pm SD ($n = 4$ mice for each condition). One-sample *t* test was performed to compare each data point with the control (no injury). *, $P < 0.05$.

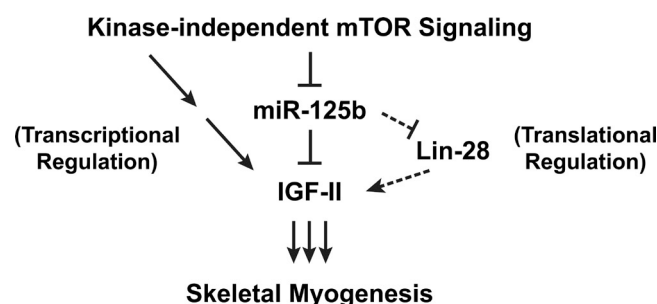


Figure 10. **A model for the regulatory network involving IGF-II in myogenesis.** Kinase-independent mTOR signaling regulates IGF-II production at a transcriptional level as well as a posttranscriptional level through miR-125b. miR-125b control of IGF-II expression may also be mediated by Lin-28 at a translational level.

Lin-28 (Fig. 10). Although our results do not rule out this possibility, they provide convincing evidence to support a direct miR-125b–IGF-II relationship: (a) miR-125b inhibits *Igf2* 3' UTR reporter activity through a seed-containing target site in HEK293 cells (Fig. 6 B), where Lin-28 is not expressed (Moss and Tang, 2003); (b) the mRNA levels of IGF-II are regulated by miR-125b in myocytes and muscles (Fig. 4, A–C; and Fig. 5), which cannot be explained by LIN-28 as a mediator because LIN-28 regulates the translation of IGF-II (Polesskaya et al., 2007).

Coordinate targeting of multiple genes in a functional pathway or protein complex has emerged as a common theme for many miRNAs (Tsang et al., 2010). For example, miR-24 coordinately targets a network of cell cycle regulators to facilitate cell cycle exit upon cellular differentiation (Lal et al., 2009); let-7 acts as a tumor suppressor by targeting multiple genes involved in cell proliferation (Johnson et al., 2007). However, in the case of miR-125b regulating myogenesis, the complete rescue of myoblast differentiation by recombinant IGF-II from the inhibitory effect of miR-125b overexpression (Fig. 4 D) is consistent with IGF-II being a major, if not the only, target of miR-125b. Although we cannot rule out the possibility of miR-125b targeting additional myogenic genes, our current observations collectively suggest that the miR-125b–IGF-II relationship is functionally dominant in the regulation of myogenesis.

As a critical inducer of skeletal myogenesis both in vitro and in vivo, it is not surprising that the myogenic production of IGF-II is tightly controlled by multiple mechanisms. The transcription of IGF-II is regulated through a muscle-specific enhancer by mTOR signaling (Erbay et al., 2003), and the translation of IGF-II during skeletal myogenesis is regulated by Lin-28 (Polesskaya et al., 2007). Our current study adds a new layer of mechanism, through an miRNA, that modulates both the mRNA and protein levels of IGF-II. It is generally believed that miRNAs play fine-tuning roles in the control of gene expression; miR-125b targeting of IGF-II in coordination with transcriptional and translational controls is a perfect example of that principle. The strong but incomplete effects of overexpressing or antagonizing miR-125b on IGF-II expression, myogenic differentiation, and muscle regeneration (Figs. 2–4) are certainly in line with the modulating nature of miR-125b. It is reasonable to speculate that miR-125b serves as a gatekeeper to suppress IGF-II expression before cells commit to differentiation, and its

reduction below the threshold level at the initiation of differentiation allows full-blown IGF-II production activated at the transcriptional and translational levels.

Almost all of the myogenic miRNAs reported thus far are up-regulated during differentiation, with the exception of miR-221/222, which have been reported to be down-regulated and negatively regulate myogenesis in quail through the previously known target p27 (Cardinali et al., 2009). Compared with miRNAs that are often drastically up-regulated during myogenesis, miR-125b is down-regulated to less dramatic degrees during both myoblast differentiation and muscle regeneration (Fig. 1), similar to the degree of changes of miR-221/222 upon C2C12 myoblast differentiation (Cardinali et al., 2009). This is consistent with the fact that miRNAs are generally very stable (Lee et al., 2003; Lund et al., 2004). Nevertheless, the partial reduction of miR-125b is apparently sufficient and necessary to allow IGF-II expression and myogenic differentiation.

Our results also raise the distinct possibility of myogenic regulation of miR-125b biogenesis at the transcriptional level rather than the maturation steps, under the control of mTOR signaling. Further dissection of mechanisms underlying miR-125b biogenesis will require identification of the regulatory elements for the two miR-125b genes. Most recently, we have discovered a myogenic pathway in which mTOR regulates miR-1 biogenesis through MyoD (Sun et al., 2010). However, mTOR regulation of miR-125b would likely be through a different mechanism because it results in the decrease of miR-125b during myogenesis, in contrast to the increase of miR-1. Until such a mechanism is delineated, we do not know how remotely or proximately mTOR lies from miR-125b in its biogenic pathway. In any event, mTOR clearly regulates the biogenesis of these two miRNAs through distinct pathways, one dependent (miR-1; Sun et al., 2010) and one independent (miR-125b) of its kinase activity. It is interesting that this kinase-independent function of mTOR controls myogenic IGF-II production at two levels: transcriptional regulation through a muscle-specific enhancer (Erbay et al., 2003) and posttranscriptional regulation through miR-125b. This dual control underlines the importance of the mTOR–IGF-II axis in the regulation of skeletal myogenesis. Whether a single noncanonical mTOR pathway controls both processes or there are two distinct kinase-independent mTOR mechanisms will be a fascinating topic for future investigation.

Materials and methods

Antibodies and other reagents

Anti-MHC (MF20) and antimyogenin (F5D) were obtained from the Developmental Studies Hybridoma Bank developed under the auspices of the Eunice Kennedy Shriver National Institute of Child Health and Human Development, National Institutes of Health and maintained by The University of Iowa Department of Biological Sciences. Antitubulin was purchased from Abcam. Anti-BrdU was purchased from Sigma-Aldrich. All secondary antibodies were obtained from Jackson ImmunoResearch Laboratories, Inc. Rapamycin was obtained from LC Laboratories. All other reagents were purchased from Sigma-Aldrich.

Cell culture and transfection

C2C12 myoblasts were maintained in DME containing 1 g/l glucose with 10% fetal bovine serum at 37°C with 7.5% CO₂. Primary myoblasts were maintained in F-10 medium supplied with 25 ng/ml bFGF and 20% fetal

bovine serum at 37°C with 7.5% CO₂. To induce differentiation, cells were plated on tissue culture plates coated with 0.2% gelatin and grown to 100% confluence for C2C12 and 60–70% confluence for primary myoblasts, changed into differentiation medium (DME containing 2% horse serum), and replenished with fresh medium daily for 3 (C2C12) or 2 d (primary myocytes). C2C12 myoblasts and myocytes were transfected using Lipofectamine 2000 (Invitrogen) for RNA duplexes. Introduction of LNAs and luciferase reporters into C2C12 cells was performed using Nucleofector (solution V, program B-032; Lonza) according to the manufacturer's recommendations. HEK293 cells were maintained in DME containing 4.5 g/l glucose with 10% fetal bovine serum at 37°C with 5% CO₂ and transfected using Polyfect (QIAGEN).

Mouse primary myoblast isolation

All animal experiments in this study followed protocols approved by the Animal Care and Use Committee at the University of Illinois at Urbana-Champaign. 5–7-d-old neonates were euthanized by cervical dislocation and rinsed in 70% ethanol and penicillin/streptomycin/Fungizone antibiotic solution. Hind leg muscles were isolated and minced in HBSS and digested in 2.4 U/ml dispase II (Roche) and 1.5 U/ml collagenase D (Roche) solution containing 2.5 mM CaCl₂ at 37°C for 2 h. Upon sequential filtering through 70- and 40- μ m cell strainers (BD), the cells were collected by centrifugation at 350 g and resuspended in F-10 culture medium. Serial plating was performed to enrich myoblasts and eliminate fibroblasts.

Mouse muscle injury and regeneration

10-wk-old male FVB mice were used in all the regeneration experiments. Muscle injury was induced by injection of BaCl₂ (50 μ l of 1.2% wt/vol in saline) into TA muscles as previously described (Ge et al., 2009). On various days AI, the mice were euthanized, and the TA muscles were collected, followed by cryosection and staining as described in the next section.

Muscle tissue cryosection and analysis

TA muscles were isolated by dissection, frozen in liquid nitrogen-cooled 2-methylbutane, and embedded in TBS tissue freezing medium (Thermo Fisher Scientific). Sections of 10- μ m thickness were made with a cryostat (Microm HM550; Thermo Fisher Scientific) at –20°C, placed on uncoated slides, and stained with hematoxylin and eosin (H&E). The stained slides were examined with a microscope (DMI 4000B; Leica) with a 10 \times dry objective (Fluotar, numerical aperture 0.4; Leica), and the brightfield images were captured at 24 bit at room temperature using a camera (RETIGA EXi; QImaging) equipped with Qcapture Pro51 software (QImaging). The images were then processed in Photoshop CS2 (Adobe), where brightness and contrast were adjusted. An area of 614,400 μ m² at the center of degenerated region of each TA muscle was selected for scoring centrally nucleated regenerating myofiber numbers and their cross section area.

Plasmids and oligonucleotides

The Igf2 3' UTR reporter was generated by inserting the entire 3' UTR of mouse *Igf2* gene into the pMIR-REPORTER vector (Applied Biosystems) downstream of the luciferase gene through MluI and Pml sites. The mutant Igf2 3' UTR reporters were created by mutating the seed region of the predicted miR-125b site (UCAGGG to AGUCCC) or miR-150 site (GUUGGGAG to CAACCCUC) by nested PCR. RNA duplexes for miRNAs and siEGFP (siRNA against EGFP) and LNA-containing oligonucleotides were custom synthesized by Integrated DNA Technology. The sequences of the LNA oligonucleotides are as follows, with LNA-modified nucleotides indicated by capital letters: anti-miR-125b, 5'-tcacaagTTAGGGTctcagga-3' (distinguishable from miR-125a by two LNA-modified nucleotides); and scramble, 5'-catgtcaTGTGTCACatctt-3'. miRIDIAN miR-125b mimic and a negative control (cel-miR-67; which has minimal sequence identity with miRNAs in human, mouse, and rat) were purchased from Thermo Fisher Scientific. Dy547-cel-miR-67 and FAM-anti-miR negative control were obtained from Thermo Fisher Scientific and Applied Biosystems, respectively.

Northern blotting

Antisense DNA oligonucleotides for miR-125b and let-7a were end labeled with γ -[³²P]ATP. The RNA Decade Maker (Applied Biosystems) was similarly radiolabeled as size markers. RNA (20 μ g per sample) was separated on 12% denaturing polyacrylamide gels, transferred to nylon membranes (GE Healthcare), and UV cross-linked. Prehybridization and hybridization with probe were performed in ULTRAhyb hybridization buffer (Applied Biosystems) at 42°C for 2 h and overnight, respectively. The membranes were then washed with 2 \times SSC and 0.1% SDS at 42°C, followed by exposure to x-ray films.

BrdU labeling

Subconfluent C2C12 myoblasts were incubated in BrdU (final concentration 10 μ M) under growth condition for 2 h and then fixed with 3.7% formaldehyde. After treatment by 4N HCl, immunostaining with anti-BrdU antibody and FITC-labeled anti-mouse IgG was carried out, and fluorescence microscopy was performed as described in Immunofluorescence microscopy and quantitative analysis of myocytes.

Western blotting

Cells were lysed in a buffer containing 50 mM Tris-HCl, pH 7.2, 150 mM NaCl, 1% NP-40, and 1% protease inhibitor cocktail (Sigma-Aldrich). The lysates were cleared by microcentrifugation at 14,000 rpm and then mixed with SDS sample buffer. Proteins were resolved on SDS-PAGE and transferred onto polyvinylidene fluoride membrane (Millipore) and incubated with various antibodies according to the manufacturer's recommendations. Detection of horseradish peroxidase-conjugated secondary antibodies was performed with Western Lightning Chemiluminescence Reagent Plus (PerkinElmer), and images were developed on x-ray films. Quantification of Western blot band intensities was performed by densitometry of x-ray images using the software ImageJ (National Institutes of Health).

Immunofluorescence microscopy and quantitative analysis of myocytes

C2C12 cells differentiated in 12-well plates were fixed and stained for MHC and DAPI as previously described (Park and Chen, 2005). The stained cells were examined with a DMI 4000B microscope with a 10 \times dry objective (Fluotar, numerical aperture 0.4), and the fluorescent images were captured at 8 bit at room temperature using a RETIGA EXi camera equipped with Qcapture Pro51 software. The images were then pseudocolored in Photoshop CS2, where brightness and contrast were adjusted. The differentiation and fusion indexes were calculated as the percentage of nuclei in MHC-positive myocytes and myotubes with at least two nuclei, respectively. Each data point was generated from at least 200 randomly chosen MHC-positive cells or myotubes.

Real-time qPCR

Mouse TA muscles were isolated, ground into powder in liquid nitrogen, and lysed in TRIZOL (Invitrogen). C2C12 cells or mouse primary myoblasts were lysed directly in TRIZOL. RNA was isolated according to the manufacturer's protocol. qRT-PCR for Igf2 mRNA was performed as previously described (Yoon and Chen, 2008). miR-125b levels were quantified using a qPCR-based TaqMan assay kit (Applied Biosystems) specifically designed for miR-125b (not miR-125a). SnoRNA-202, a commonly used mouse internal reference, was used as the internal control for normalization. We confirmed that Ct values of snoRNA-202 did not change from sample to sample in any systematic manner under all conditions.

Lentivirus-mediated RNAi

shRNAs in the pLKO.1-puro vector for knocking down mTOR and S6K1 were purchased from Sigma-Aldrich (MISSION TRC). Lentivirus packaging and testing were performed as previously described (Yoon and Chen, 2008). The Sigma-Aldrich clone IDs for the shRNA constructs used in this study are mTOR #1, NM_020009.1-7569s1c1; mTOR #2, NM_020009.1-5493s1c1; S6K1 #1, NM_028259.1-264s1c1; and S6K1 #2, NM_028259.1-616s1c1. C2C12 cells were transduced with lentiviruses in growth medium containing 8 μ g/ml polybrene and selected in 3 μ g/ml puromycin for 1 d, followed by plating into 12-well plates for differentiation.

Luciferase assays

C2C12 or HEK293 cells transfected with wild-type or mutant Igf2 3' UTR reporter were lysed in passive lysis buffer (Promega), and luciferase assays were performed using the Luciferase Assay Systems kit (Promega) according to the manufacturer's protocol.

Measurement of secreted IGF-II

Media were collected from differentiating C2C12 cultures and subjected to measurement of secreted IGF-II using the DuoSet ELISA Development System for mouse IGF-II (R&D Systems) according to the manufacturer's protocol.

Statistical analysis

All data are presented as mean \pm SD. Whenever necessary, statistical significance of the data was analyzed by performing one-sample *t* tests or paired *t* tests. The specific types of tests and the *p*-values, when applicable, are indicated in the figure legends.

Online supplemental material

Fig. S1 shows miR-1 and miR-206 levels in regenerating skeletal muscles. Fig. S2 shows that miR-125b does not affect proliferation of C2C12 cells.

Fig. S3 shows sequence alignment of mouse, rat, and human Igf2 at the predicted miR-125b targeting site. Fig. S4 shows that miR-150 does not target the 3' UTR of Igf2. Table S1 lists the predicted targets of miR-125b. Online supplemental material is available at <http://www.jcb.org/cgi/content/full/jcb.201007165/DC1>.

We thank Drs. K.V. Prasanth, S.G. Prasanth, and A. Lal and Mr. Z. Shen for helpful discussions, guidance, and technical assistance.

This work was supported by a grant to J. Chen from the National Institutes of Health/National Institute of Arthritis and Musculoskeletal and Skin Diseases (AR48914).

Submitted: 28 July 2010

Accepted: 9 December 2010

References

- Baek, D., J. Villén, C. Shin, F.D. Camargo, S.P. Gygi, and D.P. Bartel. 2008. The impact of microRNAs on protein output. *Nature*. 455:64–71. doi:10.1038/nature07242
- Bartel, D.P. 2009. MicroRNAs: target recognition and regulatory functions. *Cell*. 136:215–233. doi:10.1016/j.cell.2009.01.002
- Buckingham, M. 2001. Skeletal muscle formation in vertebrates. *Curr. Opin. Genet. Dev.* 11:440–448. doi:10.1016/S0959-437X(00)00215-X
- Bushati, N., and S.M. Cohen. 2007. microRNA functions. *Annu. Rev. Cell Dev. Biol.* 23:175–205. doi:10.1146/annurev.cellbio.23.090506.123406
- Caldwell, C.J., D.L. Matthey, and R.O. Weller. 1990. Role of the basement membrane in the regeneration of skeletal muscle. *Neuropathol. Appl. Neurobiol.* 16:225–238. doi:10.1111/j.1365-2990.1990.tb01159.x
- Callis, T.E., Z. Deng, J.F. Chen, and D.Z. Wang. 2008. Muscling through the microRNA world. *Exp. Biol. Med. (Maywood)*. 233:131–138. doi:10.3181/0709-MR-237
- Cardinali, B., L. Castellani, P. Fasanaro, A. Basso, S. Alemà, F. Martelli, and G. Falcone. 2009. MicroRNA-221 and microRNA-222 modulate differentiation and maturation of skeletal muscle cells. *PLoS One*. 4:e7607. doi:10.1371/journal.pone.0007607
- Chen, J.F., E.M. Mandel, J.M. Thomson, Q. Wu, T.E. Callis, S.M. Hammond, F.L. Conlon, and D.Z. Wang. 2006. The role of microRNA-1 and microRNA-133 in skeletal muscle proliferation and differentiation. *Nat. Genet.* 38:228–233. doi:10.1038/ng1725
- Chen, J.F., Y. Tao, J. Li, Z. Deng, Z. Yan, X. Xiao, and D.Z. Wang. 2010. microRNA-1 and microRNA-206 regulate skeletal muscle satellite cell proliferation and differentiation by repressing Pax7. *J. Cell Biol.* 190:867–879. doi:10.1083/jcb.200911036
- Crist, C.G., D. Montarras, G. Pallafacchina, D. Rocancourt, A. Cumano, S.J. Conway, and M. Buckingham. 2009. Muscle stem cell behavior is modified by microRNA-27 regulation of Pax3 expression. *Proc. Natl. Acad. Sci. USA*. 106:13383–13387. doi:10.1073/pnas.0900210106
- Erbay, E., I.H. Park, P.D. Nuzzi, C.J. Schoenherr, and J. Chen. 2003. IGF-II transcription in skeletal myogenesis is controlled by mTOR and nutrients. *J. Cell Biol.* 163:931–936. doi:10.1083/jcb.200307158
- Fingar, D.C., S. Salama, C. Tsou, E. Harlow, and J. Blenis. 2002. Mammalian cell size is controlled by mTOR and its downstream targets S6K1 and 4EBP1/eIF4E. *Genes Dev.* 16:1472–1487. doi:10.1101/gad.995802
- Florini, J.R., D.Z. Ewton, and K.A. Magri. 1991a. Hormones, growth factors, and myogenic differentiation. *Annu. Rev. Physiol.* 53:201–216. doi:10.1146/annurev.ph.53.030191.001221
- Florini, J.R., K.A. Magri, D.Z. Ewton, P.L. James, K. Grindstaff, and P.S. Rotwein. 1991b. “Spontaneous” differentiation of skeletal myoblasts is dependent upon autocrine secretion of insulin-like growth factor-II. *J. Biol. Chem.* 266:15917–15923.
- Florini, J.R., D.Z. Ewton, and S.A. Coolican. 1996. Growth hormone and the insulin-like growth factor system in myogenesis. *Endocr. Rev.* 17:481–517.
- Ge, Y., A.L. Wu, C. Warnes, J. Liu, C. Zhang, H. Kawasome, N. Terada, M.D. Boppart, C.J. Schoenherr, and J. Chen. 2009. mTOR regulates skeletal muscle regeneration in vivo through kinase-dependent and kinase-independent mechanisms. *Am. J. Physiol. Cell Physiol.* 297:C1434–C1444. doi:10.1152/ajpcell.00248.2009
- Greco, S., M. De Simone, C. Colussi, G. Zaccagnini, P. Fasanaro, M. Pescatori, R. Cardani, R. Perbellini, E. Isaia, P. Sale, et al. 2009. Common microRNA signature in skeletal muscle damage and regeneration induced by Duchenne muscular dystrophy and acute ischemia. *FASEB J.* 23:3335–3346. doi:10.1096/fj.08-128579
- Grimson, A., K.K. Farh, W.K. Johnston, P. Garrett-Engle, L.P. Lim, and D.P. Bartel. 2007. MicroRNA targeting specificity in mammals: determinants beyond seed pairing. *Mol. Cell.* 27:91–105. doi:10.1016/j.molcel.2007.06.017
- Guo, H., N.T. Ingolia, J.S. Weissman, and D.P. Bartel. 2010. Mammalian microRNAs predominantly act to decrease target mRNA levels. *Nature*. 466:835–840. doi:10.1038/nature09267
- Hwang, H.W., E.A. Wentzel, and J.T. Mendell. 2009. Cell-cell contact globally activates microRNA biogenesis. *Proc. Natl. Acad. Sci. USA*. 106:7016–7021. doi:10.1073/pnas.0811523106
- Inose, H., H. Ochi, A. Kimura, K. Fujita, R. Xu, S. Sato, M. Iwasaki, S. Sunamura, Y. Takeuchi, S. Fukumoto, et al. 2009. A microRNA regulatory mechanism of osteoblast differentiation. *Proc. Natl. Acad. Sci. USA*. 106:20794–20799. doi:10.1073/pnas.0909311106
- Johnson, C.D., A. Esquela-Kerscher, G. Stefani, M. Byrom, K. Kelnar, D. Ovcharenko, M. Wilson, X. Wang, J. Shelton, J. Shingara, et al. 2007. The let-7 microRNA represses cell proliferation pathways in human cells. *Cancer Res.* 67:7713–7722. doi:10.1158/0008-5472.CAN-07-1083
- Juan, A.H., R.M. Kumar, J.G. Marx, R.A. Young, and V. Sartorelli. 2009. Mir-214-dependent regulation of the polycomb protein Ezh2 in skeletal muscle and embryonic stem cells. *Mol. Cell.* 36:61–74. doi:10.1016/j.molcel.2009.08.008
- Krek, A., D. Grün, M.N. Poy, R. Wolf, L. Rosenberg, E.J. Epstein, P. MacMenamin, I. da Piedade, K.C. Gunsalus, M. Stoffel, and N. Rajewsky. 2005. Combinatorial microRNA target predictions. *Nat. Genet.* 37:495–500. doi:10.1038/ng1536
- Lagos-Quintana, M., R. Rauhut, A. Yalcin, J. Meyer, W. Lendeckel, and T. Tuschl. 2002. Identification of tissue-specific microRNAs from mouse. *Curr. Biol.* 12:735–739. doi:10.1016/S0960-9822(02)00809-6
- Lal, A., F. Navarro, C.A. Maher, L.E. Maliszewski, N. Yan, E. O’Day, D. Chowdhury, D.M. Dykxhoorn, P. Tsai, O. Hofmann, et al. 2009. miR-24 Inhibits cell proliferation by targeting E2F2, MYC, and other cell-cycle genes via binding to “seedless” 3’UTR microRNA recognition elements. *Mol. Cell.* 35:610–625. doi:10.1016/j.molcel.2009.08.020
- Lassar, A., and A. Münsterberg. 1994. Wiring diagrams: regulatory circuits and the control of skeletal myogenesis. *Curr. Opin. Cell Biol.* 6:432–442. doi:10.1016/0955-0674(94)90037-X
- Le, M.T., C. Teh, N. Shyh-Chang, H. Xie, B. Zhou, V. Korzh, H.F. Lodish, and B. Lim. 2009a. MicroRNA-125b is a novel negative regulator of p53. *Genes Dev.* 23:862–876. doi:10.1101/gad.1767609
- Le, M.T., H. Xie, B. Zhou, P.H. Chia, P. Rizk, M. Um, G. Udolph, H. Yang, B. Lim, and H.F. Lodish. 2009b. MicroRNA-125b promotes neuronal differentiation in human cells by repressing multiple targets. *Mol. Cell Biol.* 29:5290–5305. doi:10.1128/MCB.01694-08
- Lee, R.C., R.L. Feinbaum, and V. Ambros. 1993. The *C. elegans* heterochronic gene lin-4 encodes small RNAs with antisense complementarity to lin-14. *Cell*. 75:843–854. doi:10.1016/0092-8674(93)90529-Y
- Lee, Y., C. Ahn, J. Han, H. Choi, J. Kim, J. Yim, J. Lee, P. Provost, O. Rådmark, S. Kim, and V.N. Kim. 2003. The nuclear RNase III Drosha initiates microRNA processing. *Nature*. 425:415–419. doi:10.1038/nature01957
- Lewis, B.P., C.B. Burge, and D.P. Bartel. 2005. Conserved seed pairing, often flanked by adenosines, indicates that thousands of human genes are microRNA targets. *Cell*. 120:15–20. doi:10.1016/j.cell.2004.12.035
- Lund, E., S. Güttinger, A. Calado, J.E. Dahlberg, and U. Kutay. 2004. Nuclear export of microRNA precursors. *Science*. 303:95–98. doi:10.1126/science.1090599
- McArdle, A., R.H. Edwards, and M.J. Jackson. 1994. Release of creatine kinase and prostaglandin E2 from regenerating skeletal muscle fibers. *J. Appl. Physiol.* 76:1274–1278.
- Moss, E.G., and L. Tang. 2003. Conservation of the heterochronic regulator Lin-28, its developmental expression and microRNA complementary sites. *Dev. Biol.* 258:432–442. doi:10.1016/S0012-1606(03)00126-X
- Moss, E.G., R.C. Lee, and V. Ambros. 1997. The cold shock domain protein LIN-28 controls developmental timing in *C. elegans* and is regulated by the lin-4 RNA. *Cell*. 88:637–646. doi:10.1016/S0092-8674(00)81906-6
- Naguibneva, I., M. Ameyar-Zazoua, N. Nonne, A. Poleskaya, S. Ait-Si-Ali, R. Groisman, M. Souidi, L.L. Pritchard, and A. Harel-Bellan. 2006a. An LNA-based loss-of-function assay for micro-RNAs. *Biomed. Pharmacother.* 60:633–638. doi:10.1016/j.biopha.2006.07.078
- Naguibneva, I., M. Ameyar-Zazoua, A. Poleskaya, S. Ait-Si-Ali, R. Groisman, M. Souidi, S. Cuvellier, and A. Harel-Bellan. 2006b. The microRNA miR-181 targets the homeobox protein Hox-A11 during mammalian myoblast differentiation. *Nat. Cell Biol.* 8:278–284. doi:10.1038/ncb1373
- Naya, F.J., and E. Olson. 1999. MEF2: a transcriptional target for signaling pathways controlling skeletal muscle growth and differentiation. *Curr. Opin. Cell Biol.* 11:683–688. doi:10.1016/S0955-0674(99)00036-8
- O’Rourke, J.R., S.A. Georges, H.R. Seay, S.J. Tapscott, M.T. McManus, D.J. Goldhamer, M.S. Swanson, and B.D. Harfe. 2007. Essential role for Dicer during skeletal muscle development. *Dev. Biol.* 311:359–368. doi:10.1016/j.ydbio.2007.08.032

- Paoni, N.F., F. Peale, F. Wang, C. Errett-Baroncini, H. Steinmetz, K. Toy, W. Bai, P.M. Williams, S. Bunting, M.E. Gerritsen, and L. Powell-Braxton. 2002. Time course of skeletal muscle repair and gene expression following acute hind limb ischemia in mice. *Physiol. Genomics*. 11:263–272.
- Park, I.H., and J. Chen. 2005. Mammalian target of rapamycin (mTOR) signaling is required for a late-stage fusion process during skeletal myotube maturation. *J. Biol. Chem.* 280:32009–32017. doi:10.1074/jbc.M506120200
- Parker, M.H., P. Seale, and M.A. Rudnicki. 2003. Looking back to the embryo: defining transcriptional networks in adult myogenesis. *Nat. Rev. Genet.* 4:497–507. doi:10.1038/nrg1109
- Perry, R.L.S., and M.A. Rudnick. 2000. Molecular mechanisms regulating myogenic determination and differentiation. *Front. Biosci.* 5:D750–D767. doi:10.2741/Perry
- Polesskaya, A., S. Cuvellier, I. Naguibneva, A. Duquet, E.G. Moss, and A. Harel-Bellan. 2007. Lin-28 binds IGF-2 mRNA and participates in skeletal myogenesis by increasing translation efficiency. *Genes Dev.* 21:1125–1138. doi:10.1101/gad.415007
- Rosen, K.M., B.M. Wentworth, N. Rosenthal, and L. Villa-Komaroff. 1993. Specific, temporally regulated expression of the insulin-like growth factor II gene during muscle cell differentiation. *Endocrinology*. 133:474–481. doi:10.1210/en.133.2.474
- Shin, C., J.-W. Nam, K.K.-H. Farh, H.R. Chiang, A. Shkumatava, and D.P. Bartel. 2010. Expanding the microRNA targeting code: functional sites with centered pairing. *Mol. Cell.* 38:789–802. doi:10.1016/j.molcel.2010.06.005
- Small, E.M., J.R. O'Rourke, V. Moresi, L.B. Sutherland, J. McAnally, R.D. Gerard, J.A. Richardson, and E.N. Olson. 2010. Regulation of PI3-kinase/Akt signaling by muscle-enriched microRNA-486. *Proc. Natl. Acad. Sci. USA.* 107:4218–4223. doi:10.1073/pnas.1000300107
- Stark, A., J. Brennecke, R.B. Russell, and S.M. Cohen. 2003. Identification of *Drosophila* MicroRNA targets. *PLoS Biol.* 1:E60. doi:10.1371/journal.pbio.0000060
- Sun, Q., Y. Zhang, G. Yang, X. Chen, Y. Zhang, G. Cao, J. Wang, Y. Sun, P. Zhang, M. Fan, et al. 2008. Transforming growth factor-beta-regulated miR-24 promotes skeletal muscle differentiation. *Nucleic Acids Res.* 36:2690–2699. doi:10.1093/nar/gkn032
- Sun, Y., Y. Ge, J. Drnevich, Y. Zhao, M. Band, and J. Chen. 2010. Mammalian target of rapamycin regulates miRNA-1 and follistatin in skeletal myogenesis. *J. Cell Biol.* 189:1157–1169. doi:10.1083/jcb.200912093
- Tsang, J.S., M.S. Ebert, and A. van Oudenaarden. 2010. Genome-wide dissection of microRNA functions and cotargeting networks using gene set signatures. *Mol. Cell.* 38:140–153. doi:10.1016/j.molcel.2010.03.007
- van Rooij, E., D. Quiat, B.A. Johnson, L.B. Sutherland, X. Qi, J.A. Richardson, R.J. Kelm Jr., and E.N. Olson. 2009. A family of microRNAs encoded by myosin genes governs myosin expression and muscle performance. *Dev. Cell.* 17:662–673. doi:10.1016/j.devcel.2009.10.013
- Wagers, A.J., and I.M. Conboy. 2005. Cellular and molecular signatures of muscle regeneration: current concepts and controversies in adult myogenesis. *Cell.* 122:659–667. doi:10.1016/j.cell.2005.08.021
- Wang, H., R. Garzon, H. Sun, K.J. Ladner, R. Singh, J. Dahlman, A. Cheng, B.M. Hall, S.J. Qualman, D.S. Chandler, et al. 2008. NF-kappaB-YY1-miR-29 regulatory circuitry in skeletal myogenesis and rhabdomyosarcoma. *Cancer Cell.* 14:369–381. doi:10.1016/j.ccr.2008.10.006
- Weintraub, H. 1993. The MyoD family and myogenesis: redundancy, networks, and thresholds. *Cell.* 75:1241–1244. doi:10.1016/0092-8674(93)90610-3
- Williams, A.H., N. Liu, E. van Rooij, and E.N. Olson. 2009. MicroRNA control of muscle development and disease. *Curr. Opin. Cell Biol.* 21:461–469. doi:10.1016/j.ceb.2009.01.029
- Wong, C.F., and R.L. Tellam. 2008. MicroRNA-26a targets the histone methyltransferase Enhancer of Zeste homolog 2 during myogenesis. *J. Biol. Chem.* 283:9836–9843. doi:10.1074/jbc.M709614200
- Wu, L., and J.G. Belasco. 2005. Micro-RNA regulation of the mammalian lin-28 gene during neuronal differentiation of embryonal carcinoma cells. *Mol. Cell Biol.* 25:9198–9208. doi:10.1128/MCB.25.21.9198-9208.2005
- Wu, L., J. Fan, and J.G. Belasco. 2006. MicroRNAs direct rapid deadenylation of mRNA. *Proc. Natl. Acad. Sci. USA.* 103:4034–4039. doi:10.1073/pnas.0510928103
- Yoon, M.S., and J. Chen. 2008. PLD regulates myoblast differentiation through the mTOR-IGF2 pathway. *J. Cell Sci.* 121:282–289. doi:10.1242/jcs.022566

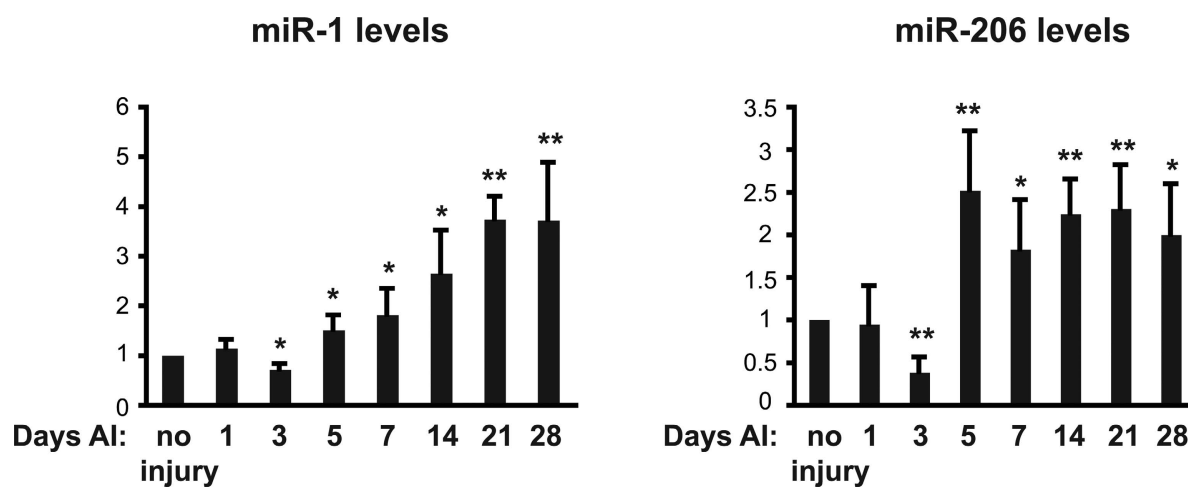
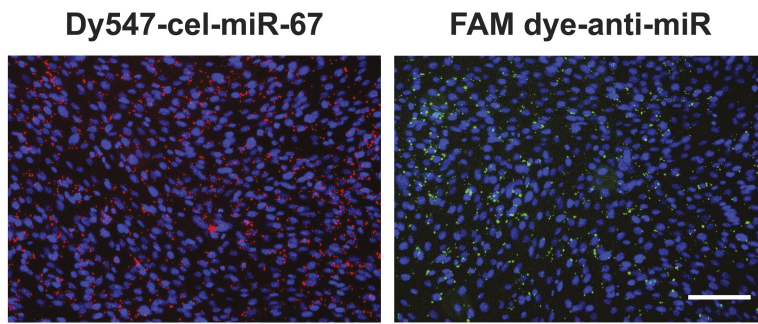
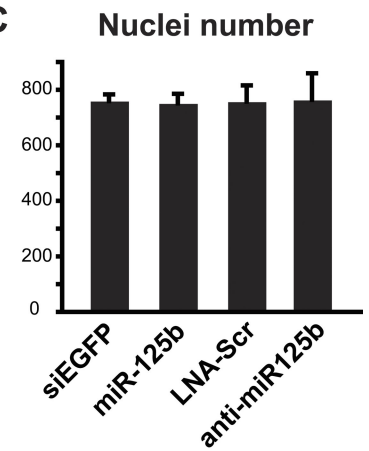
Ge et al., <http://www.jcb.org/cgi/content/full/jcb.201007165/DC1>

Figure S1. **miR-1 and miR-206 levels in regenerating skeletal muscles.** Regeneration of TA muscles in mouse was induced by BaCl₂ injury. On various days AI, total RNA was isolated from the TA muscles and subjected to analysis by qRT-PCR to determine the relative levels of miR-1 and miR-206. Saline injection into contralateral TA muscles served as “no injury” control. The data shown are mean \pm SD with three mice per time point. One-sample *t* test was performed to compare each data point with the control (no injury). *, $P < 0.05$; **, $P < 0.01$.

A



C



B

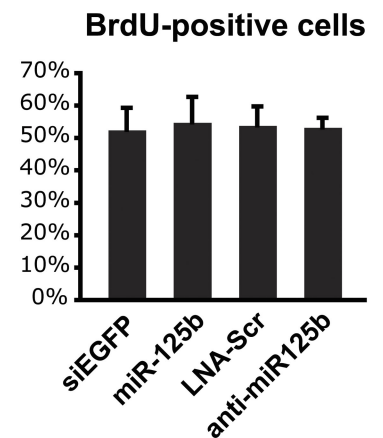
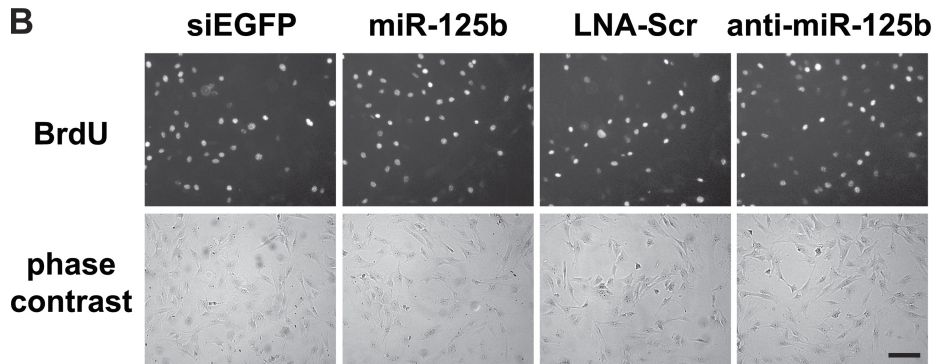


Figure S2. **miR-125b does not affect proliferation of C2C12 cells.** (A) Efficiencies for delivering double- and single-stranded oligonucleotides into C2C12 cells were assessed by transfection of 50 nM Dy547-cel-miR-67 (red) and FAM dye-anti-miR (green), respectively. DAPI staining is shown in blue. The granular appearance of transfected oligonucleotides is commonly seen with C2C12 cells (Technical Notes; Thermo Fisher Scientific). (B) C2C12 myoblasts were transfected with various oligonucleotides as indicated. After 24 h, BrdU labeling was performed as described in Materials and methods. The percentage of BrdU-positive cells was quantified. (C) Cell density at the end of 3-d differentiation described in Fig. 2 was assessed by counting nuclear number per 614,400-µm² view. Data shown are mean ± SD from three independent experiments. Bars, 100 µm.



Figure S3. **Sequence alignment of mouse, rat, and human Igf2 at the predicted miR-125b targeting site.** Sequence in red is in the seed region. Mismatched bases among the three Igf2 sequences are indicated as follows: blue, loss of pairing with miR-125b; green, no effect on miR-125b pairing; purple, gain of pairing with miR-125b. The miR-125b sequence is identical in all species.

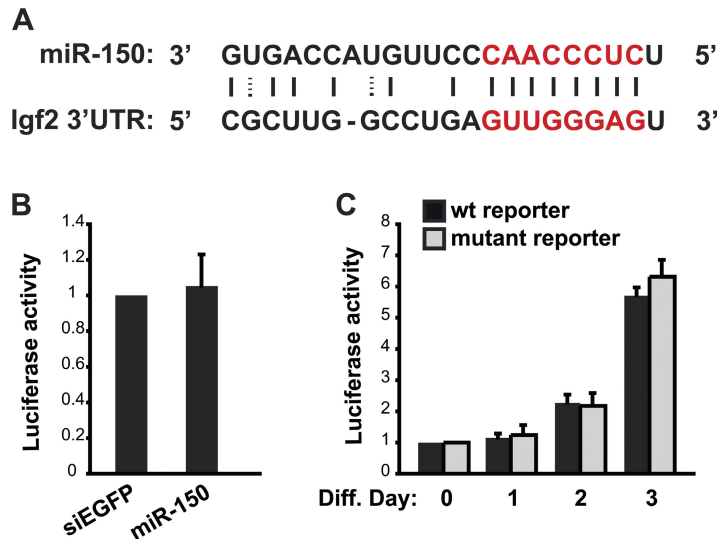


Figure S4. **miR-150 does not target the 3' UTR of Igf2.** (A) Predicted miR-150 target site in the 3' UTR of mouse Igf2. The seed region is indicated in red. Solid and dashed vertical lines indicate Watson-Crick base pairing and wobble base pairing, respectively. (B) HEK293 cells were transfected with the Igf2 3' UTR reporter together with siEGFP or miR-150 duplex. The cells were lysed 24 h later and subjected to luciferase assays. (C) C2C12 myoblasts were transfected with the Igf2 3' UTR reporter or its miR-150 site mutant and then induced to differentiate for up to 3 d. The cells were lysed at the indicated times, and luciferase assays were performed. The mean results of three independent experiments are shown, with error bars representing SD. Diff., differentiation; wt, wild type.

Table S1. **Predicted targets of miR-125b**

GenBank accession number	Gene symbol	Full gene name	Number of sites	Prediction algorithm
NM_009530	<i>Atrx</i>	α thalassemia/mental retardation syndrome X-linked homologue	1	miRanda
NM_145959	<i>D15Ert621e</i>	DNA segment, Chr 15, ERATO Doi 621, expressed	1	miRanda
NM_029352	<i>Dusp9</i>	Dual specificity phosphatase 9	1	miRanda
NM_138677	<i>Edem1</i>	ER degradation enhancer, mannosidase α -like 1	1	TargetScan
NM_008251	<i>Hmgn1</i>	High mobility group nucleosomal binding domain 1	1	miRanda
NM_010514	<i>Igf2</i>	Insulin-like growth factor II	1	miRanda
NM_008538	<i>Marcks</i>	Myristoylated alanine-rich protein kinase C substrate	1	miRanda
NM_026758	<i>Mphosph6</i>	M phase phosphoprotein 6	1	miRanda
NM_183355	<i>Pbx1</i>	Pre B-cell leukemia transcription factor 1	1	miRanda
NM_019547	<i>Rbm38</i>	RNA-binding motif protein 38	1	TargetScan
NM_011514	<i>Suv39h1</i>	Suppressor of variegation 3-9 homologue 1	1	miRanda, TargetScan, and PicTar

Listed are genes that were predicted to be miR-125b targets by one of the three algorithms and up-regulated during C2C12 differentiation (Park and Chen, 2005). The genes are listed in alphabetical order of gene symbol. Accession numbers are available from GenBank/EMBL/DDBJ. The prediction programs used were miRanda (<http://www.microRNA.org>, January 2008 release), TargetScan (mouse 4.2 version, April 2008), and PicTar (a single version available).

Reference

Park, I.H., and J. Chen. 2005. Mammalian target of rapamycin (mTOR) signaling is required for a late-stage fusion process during skeletal myotube maturation. *J. Biol. Chem.* 280:32009–32017. doi:10.1074/jbc.M506120200